ICARUS 102, 316–332 (1993)

Secular Resonances in Mean Motion Commensurabilities: The 2/1 and 3/2 Cases

ALESSANDRO MORBIDELLI[1]
Département de mathématique FUNDP, Namur, Belgium

AND

MICHELE MOONS[2]
Département de mathématique FUNDP, Namur, Belgium

Received September 4, 1992; revised January 8, 1993

The dynamic behavior of asteroids orbiting near the mean motion commensurabilities 2/1 and 3/2 with Jupiter is strongly affected by secular perturbations due to the outer planets, which are not present in the usual models based on the restricted three-body problem. Moreover, many interesting and puzzling phenomena involve inclined asteroid orbits and cannot be studied by planar models. Therefore, we have investigated the location and the dynamic effects of the three main secular resonances ν_5, ν_6, and ν_{16}, *inside* the mean motion commensurabilities. This is done by means of a seminumerical method, which allows us to obtain a 3-D picture of the dynamics, including the case of asteroids at high inclinations. Our findings throw new light on the existence of the Hecuba gap and the Hilda group in the asteroid belt. In particular, we have found that: (i) The interaction between the ν_5 and the ν_6 resonances gives rise to large chaotic zones for eccentricities >0.25 and >0.45 in the 3/2 and 2/1 resonances, respectively, which may cause close encounters with Jupiter and ejection from the solar system—however, the Hilda asteroids avoid this chaotic zone due to a phase-related protection mechanism. (ii) At large eccentricities the resonance causing a libration of the argument of perihelion is also present and can force strong secular changes of the eccentricity and the inclination. (iii) Although the Hilda group is bounded below the ν_{16} resonance curve in the inclination vs. eccentricity plane, such a boundary is not present in the 2/1 resonance, where ν_{16} affects zero-inclination orbits at eccentricities of about 0.2. However, this resonance can substantially increase the inclination but not the eccentricity and does not affect nearly circular orbits; therefore its location is not sufficient to explain the formation of the Hecuba gap.

1. INTRODUCTION

The motion of asteroids in mean motion commensurabilities with Jupiter has been studied many times, and extensive references on this subject can be found in Yoshikawa (1989) and in Henrard (1988). Here we aim to revisit this problem under at least three new aspects: by using a more realistic model which includes the perturbations of the Jupiter–Saturn system, by extending our analysis to the orbits with nonzero inclination, and by developing a general theory which can be applied directly to any mean motion resonance. This first paper is devoted to the case of the 2/1 and 3/2 mean motion commensurabilities.

For what concerns the model, all theoretical work about the dynamics in mean motion resonances has been carried out up to now in the framework of the restricted three-body problem. This is probably due to historical reasons, since this was the model adopted first by Poincaré (1892). Although this model is suitable for pointing out many features of the resonant dynamics, it is not a realistic one for describing the dynamics in the asteroid belt. Indeed, Jupiter's orbit is not a Keplerian one; it changes with time, under the perturbation of the other planets, mainly Saturn. This movement, although very slow, is not negligible, even from a qualitative point of view, since it introduces new secular frequencies; by consequence, a new class of resonances, called secular resonances, can occur, changing completely the dynamic picture.

In particular, three secular resonances are very important: ν_5, ν_6, and ν_{16}. The ν_5 and the ν_6 resonances are given by the 1/1 commensurabilities between the frequency of the longitude of perihelion of the asteroid and one of the two main characteristic frequencies of the motion of Jupiter's longitude of perihelion, g_5 and g_6, respec-

[1] Current address: Observatoire de la Côte d'Azur, B.P. 229, 06304 Nice Cedex 4, France.

[2] Current address: Département de mathématique FUNDP, 8, Rempart de la Vierge, 5000 Namur, Belgium.

0019-1035/93 $5.00

tively. The ν_{16} resonance is the corotation of the node of the asteroid with that of Jupiter. In the restricted three-body problem, the ν_5 secular resonance is approximated by the resonance that occurs when the frequency of the asteroid's perihelion is locked around zero. Notably, this resonance is at the origin of the phenomena which are claimed by Wisdom (1983, 1985) and Yoshikawa (1989, 1991) to explain the existence of gaps in the distribution of the asteroids in correspondence with the 3/1, 4/1, and 5/2 mean motion commensurabilities. Conversely, the ν_6 and the ν_{16} secular resonances are completely absent in the framework of the three-body problem.

It is well known now that, far from mean motion commensurabilities, the structure of the asteroid belt is determined by the presence of secular resonances. These have been extensively studied by Williams (1969), Williams and Faulkner (1981), Nakai and Kinoshita (1985), Yoshikawa (1987), Morbidelli and Henrard (1991), Knežević *et al.* (1991), and all modern quantitative theories for the computation of asteroid proper elements take into account the slow secular changes in the orbit of Jupiter (see Lemaître 1992). Therefore, with this work, we wish to update our knowledge on mean motion commensurabilities by adopting the same model used for the computation of asteroid proper elements; in particular we look for the existence of secular resonances inside mean motion commensurabilities and study their dynamic effect. This will provide some nice surprises.

The use of a more realistic model forces us to take into account also the motion at nonzero inclination. In the framework of the restricted three-body problem, the dynamics is symmetric with respect to the orbital plane of the perturbing body; therefore if the asteroid's orbit has initially a zero inclination, it will never leave such a plane. This is no longer true in the framework of the more realistic model in which Jupiter's inclination is nonzero and its longitude of node is precessing: no constant value of inclination is possible a priori.

Very few analytic works exist on the dynamics in mean motion commensurabilities in three dimensions ($i \neq 0$). Yoshikawa's work (1989, 1991), in principle, is not limited to the case $i = 0$, but the problem is oversimplified by averaging the equations of motion over the argument of perihelion. Such a simplification cannot be supported by any perturbation scheme, since a resonance in the motion of the argument of perihelion occurs, as pointed out by Morbidelli and Giorgilli (1990). This last work, however, does not provide a global picture of the dynamics, but only locates periodic orbits; moreover it is also carried out in the framework of the restricted three-body problem.

In our study, we do not restrict ourselves to small values of the eccentricity e and the inclination i. This is mainly due to the fact that the secular perturbations may force eccentricity and inclination to quite large values. Therefore, instead of dealing with classical series expansions in e and i, we will evaluate the Hamiltonian and its derivatives in closed form, following Ferraz-Mello and Sato (1989) and Morbidelli and Giorgilli (1990). We believe that this approach obtains results consistent everywhere in the space.

For what concerns the perturbation approach, we pay lot of care in developing a theory suitable for exploring any mean motion commensurability, avoiding all ad-hoc simplifications and adaptations. This is achieved by introducing suitable action–angle variables in a seminumerical way, following Henrard (1990), and implementing, when necessary, the algorithm of successive elimination of the harmonics (Morbidelli 1992). This fact is probably more important from the mathematical point of view, rather than for what concerns the physical results. However, a unitary theory allows the similarities among mean motion commensurabilities and the particularities of some of them to be pointed out better. Therefore we hope that this will allow a better comparative understanding of the dynamics in the asteroid belt.

In this paper we concentrate our attention on the dynamics in the 2/1 and 3/2 mean motion commensurabilities. These are in some sense the most mysterious ones. Indeed all studies performed in the framework of the three-body problem point out that the two resonances have very similar dynamic behaviors. Despite that, the 3/2 resonance hosts a family of asteroids, called the Hildas, whereas the 2/1 one is associated to a puzzling gap (the Hecuba gap), where asteroids are absent (apart from very few exceptions). A possible explanation of this fact lies in the cosmogonic scenario by Henrard and Lemaître (1983b). Therefore, a challenge exists to explain the Hecuba gap on the base of the resonant dynamics, taking into account only gravitational forces.

We anticipate here our main results:

(1) The interaction between the ν_5 and the ν_6 secular resonances causes the existence of a very wide chaotic zone at large eccentricity ($e > 0.25$) in the 3/2 and at very large eccentricity ($e > 0.45$) in the 2/1. In the latter case escape from the Solar System may occur. The Hilda asteroids seem to avoid such a chaotic zone, since they are phase-protected.

(2) The resonance of the argument of perihelion, which causes important excursions of the eccentricity and the inclination, is also present at large eccentricity ($e \sim 0.4$ in the 3/2 and $e \sim 0.7$ in the 2/1).

(3) The ν_{16} secular resonance bounds the Hilda family in the (e, i) plane in the 3/2 commensurability (see Fig. 14). Conversely, in the 2/1 mean motion commensurability, it is present at moderate eccentricity: it cuts the plane $i = 0$ at $e \sim 0.2$. Therefore, if the Hilda family

were translated into the 2/1 commensurability (i.e., changing the semimajor axis, but not the eccentricity and the inclination) it would be crossed by this secular resonance, the effect of which is to considerably increase the inclination.

However, we do not claim to have solved the problem of the formation of the Kirkwood gaps in a noncosmogonic way. Indeed, the ν_{16} resonance in the 2/1 commensurability seems to be isolated from the resonance of the argument of perihelion and from the other main secular resonances; therefore the resonant motion looks regular and, even if the inclination can increase to 30°, the eccentricity does not show important changes. This has been confirmed by a numerical simulation over 1.5 Myr. Moreover, if the initial eccentricity is smaller than 0.15 and the inclination is low, fictitious asteroids may avoid the ν_{16} resonance. On the other hand, it is difficult to believe that the existence of this secular resonance, which is the only important difference we have found between the 2/1 and 3/2 case, does not have a role in the existence of the Hecuba gap. The fact that it bounds the asteroids' distribution in the Hilda family, suggests that this secular resonance *is* dynamically important, even if we do not understand well how. One could conjecture the existence of slow Arnold diffusion at large inclination, whereto the asteroids are pushed by the ν_{16} resonance; such a diffusion could be produced by the presence of secondary resonances of higher order and could make the eccentricity increase to large values so that the asteroid becomes a planet crosser. Of course proving this conjecture goes beyond our analytic possibilities. A specific numerical research in this direction should be interesting; however, the timescales being very long, this would not be an easy job.

The paper is structured as follows. Section 2 is devoted to the general settings and to the perturbation approach used in this work; it is the mathematical section of the paper. Those who are interested only in the physical results on the dynamics in 2/1 and 3/2 resonances can skip it and go directly to the specific Sections 3 and 4.

2. GENERAL SETTINGS AND PERTURBATION SCHEME

This section is devoted to the presentation of the mathematical background of our theory. As guiding line, we follow the philosophy of the successive elimination of perturbation harmonics (Morbidelli 1992), searching and eliminating, one after the other, the most important harmonics in the different regions of the phase space. This leads us to determine the geography of the main resonances and to build up local adaptative (quasi-integrable) models to describe the main features of the dynamics.

In what follows, we shall adopt the usual notations for the Keplerian elements of the asteroid (resp. Jupiter): a (resp. a') for the semimajor axis, e (resp. e') for the eccentricity, i (resp. i') for the inclination, λ (resp. λ') for the mean longitude, $\tilde{\omega}$ (resp. $\tilde{\omega}'$) for the longitude of perihelion, and Ω (resp. Ω') for the longitude of node.

We start with the Hamiltonian of the restricted three-body problem Sun–Jupiter–asteroid (see, for instance, Szebehely 1967)

$$\mathcal{H} = L' - \frac{1-\mu}{2a} - \mu\left(\frac{1}{|\mathbf{r}-\mathbf{r}'|} - \frac{\mathbf{r}|\mathbf{r}'}{r'^3}\right),$$

where $\mathbf{r}$ is the heliocentric position vector of the asteroid, $\mathbf{r}'$ the one of Jupiter, μ the mass of Jupiter, and L' the conjugate momentum to the mean longitude of Jupiter. The universal gravitational constant, the semimajor axis of Jupiter, and the total mass of the Sun–Jupiter system are chosen as units.

We immediately extend the problem in order to take into account the secular variations of the orbital elements of Jupiter due to the presence of the other planets (mainly Saturn):

$$\begin{aligned} e'\cos\tilde{\omega}' &= m_{5,5}\cos(g_5 t + \lambda_5^0) + m_{5,6}\cos(g_6 t + \lambda_6^0) \\ e'\sin\tilde{\omega}' &= m_{5,5}\sin(g_5 t + \lambda_5^0) + m_{5,6}\sin(g_6 t + \lambda_6^0) \\ \sin i'/2\cos\Omega' &= n_{5,6}\cos(s_6 t + \mu_6^0) \\ \sin i'/2\sin\Omega' &= n_{5,6}\sin(s_6 t + \mu_6^0). \end{aligned} \tag{1}$$

The adopted values for the constants $m_{5,5}$, g_5, λ_5^0, $m_{5,6}$, g_6, λ_6^0, $n_{5,6}$, s_6, and μ_6^0 are taken from the LONGSTOP numerical integration of the outer Solar System (Nobili *et al.*, 1989): $g_5 = 4.2575''/y$, $g_6 = 28.2455''/y$, $s_6 = -26.3450''/y$, $\lambda_5^0 = 27.0°$, $\lambda_6^0 = 124.2°$, $\mu_6^0 = 304.0°$, $m_{5,5} = 4.419 \times 10^{-2}$, $m_{5,6} = -1.570 \times 10^{-2}$, $n_{5,6} = 3.153 \times 10^{-3}$.

With the introduction of resonance variables appropriate to the $(p+q)/p$ mean motion resonance and the introduction of three new momenta conjugated to the three new time dependances introduced by the Jupiter–Saturn system, the seven-degree-of-freedom autonomous Hamitonian of the problem reads

$$\begin{aligned} \mathcal{H} = \Lambda' + g_5\Lambda_5' + g_6\Lambda_6' + s_6\Lambda_{16}' - \frac{p+q}{p}L - \frac{1-\mu}{2a} \\ - \mu\left(\frac{1}{|\mathbf{r}-\mathbf{r}'|} - \frac{\mathbf{r}|\mathbf{r}'}{r'^3}\right), \end{aligned} \tag{2}$$

the phase space being described by the variables

$$
\begin{aligned}
\sigma &= \frac{p+q}{q}\lambda' - \frac{p}{q}\lambda - \tilde{\omega}, & S &= L - G \\
\sigma_z &= \frac{p+q}{q}\lambda' - \frac{p}{q}\lambda - \Omega, & S_z &= G - H \\
-\nu &= \frac{p+q}{q}\lambda' - \frac{p}{q}\lambda, & N &= \frac{p+q}{p}L - H \\
&\lambda', & \Lambda' &= \frac{p+q}{p}L + L' \qquad (3) \\
\tilde{\omega}'_5 &\equiv g_5 t, & &\Lambda'_5 \\
\tilde{\omega}'_6 &\equiv g_6 t, & &\Lambda'_6 \\
\Omega' &\equiv s_6 t, & &\Lambda'_{16},
\end{aligned}
$$

where $L = \sqrt{(1-\mu)a}$, $G = L\sqrt{1-e^2}$, and $H = G\cos i$ are the usual Delaunay's momenta.

Our aim is now to reduce the number of degrees of freedom in order to be able to study the dynamics associated to such an Hamiltonian. The first step will consist of the averaging of the Hamiltonian with respect to the mean longitude of Jupiter in order to remove from the problem all of the short periodic oscillations. This averaging is done by a numerical process. Indeed, it is worth noting here that, in the computation of the Hamiltonian (2), we do not perform the classical developments in power series of the eccentricity and the inclination of the asteroid nor in Fourier series of the angular variables. The value of the Hamiltonian (and of its derivatives when needed) is computed for any given value of the phase space variables using closed formulas which are nonsingular at low eccentricity and/or inclination and remain valid at high values of both quantities (Ferraz-Mello and Sato 1989). The motion of the asteroid is thus described very precisely, without any restriction about the size of the eccentricity or of the inclination. The dependence on Jupiter, on the contrary, is truncated at the first order in the eccentricity and inclination as the maximum value of those quantities is always small. We know, however (see Moons and Morbidelli 1992), that higher order terms in e' are responsible for the existence of small chaotic layers at moderate eccentricity.

After the elimination of the short periodic terms, the Hamiltonian is still a six-degree-of-freedom one. In any case, there is a hierarchy among the degrees of freedom; indeed, we can divide the Hamiltonian into a main part, independent of e' and i', and a perturbation given by the linear terms in e' and i'. However, the main part is not integrable since it depends on the two angles σ and σ_z. In a first step, we shall thus study the planar problem ($i = i' = 0$), the main part of which is integrable as it depends on the angle σ only. After that, we will extend the theory to the three-dimensional case.

2.1. The Planar Problem

The planar problem ($i = i' = 0$) is a four-degree-of-freedom problem independent of the variables σ_z, S_z, Ω', and Λ'_{16}. The Hamiltonian of this problem can be written

$$\mathcal{H} = g_5\Lambda'_5 + g_6\Lambda'_6 + \mathcal{H}_0(\sigma, S, N) + \mathcal{H}_1, \qquad (4)$$

where $\mathcal{H}_0(\sigma, S, N)$ is integrable and where the perturbation $\mathcal{H}_1$ contains all the terms proportional to e':

$$\mathcal{H}_1 = m_{5,5}\mathcal{H}_{1,5}(\sigma, S, \nu, N, \tilde{\omega}'_5) + m_{5,6}\mathcal{H}_{1,6}(\sigma, S, \nu, N, \tilde{\omega}'_6). \qquad (5)$$

The integrable part $\mathcal{H}_0(\sigma, S, N)$ can be viewed as a one-degree-of-freedom Hamiltonian in (σ, S) depending on a parameter N. The phase space of this Hamiltonian (see Fig. 1) has been studied many times in the past for low values of the eccentricity (see, for instance, Henrard and Lemaître 1983a, Lemaître 1984). Its shape at high eccentricity is described in (Moons and Morbidelli 1992) and is somewhat different: the size of the maximal excursion in eccentricity along a librating trajectory is reduced and, for the 2/1 and 3/2 resonances, a new stable family of periodic orbits of the nonaveraged problem appears at $\sigma = \pi$.

In any case, the dynamics associated with $\mathcal{H}_0$ are far from being trivial and, in order to simplify the expression of $\mathcal{H}_0$ while taking into account the full distortion of its invariant tori, without any approximation, we shall introduce suitable Arnold action–angle variables. These are defined in order that the new actions J and J' are constants of motion for $\mathcal{H}_0$ (i.e., their values parametrize the invariant tori which the phase space is foliated into) and the new angles ψ and ψ' are linear functions of the time. The transformation from (σ, S, ν, N) to (ψ, J, ψ', J') is given by (see Henrard, 1990)

$$
\begin{aligned}
\psi &= \frac{2\pi}{T}t, & J &= \frac{1}{2\pi}\oint S\,d\sigma \\
\psi' &= \nu - \rho(\psi, J, J'), & J' &= N,
\end{aligned}
\qquad (6)
$$

where the integral is computed along a periodic orbit in (σ, S) of $\mathcal{H}_0$ and where t is the time, T the period of the orbit, and ρ a periodic function. We stress that such a transformation is not an explicit one; on the other hand, as shown in Henrard (1990), we are able to handle the new variables by computing them numerically on each desired torus. We do not insist on the technical details of this procedure, since they have already been discussed in many papers (see, for instance, Morbidelli and Henrard 1991, Moons and Henrard 1992, Lemaître and Morbidelli 1992).

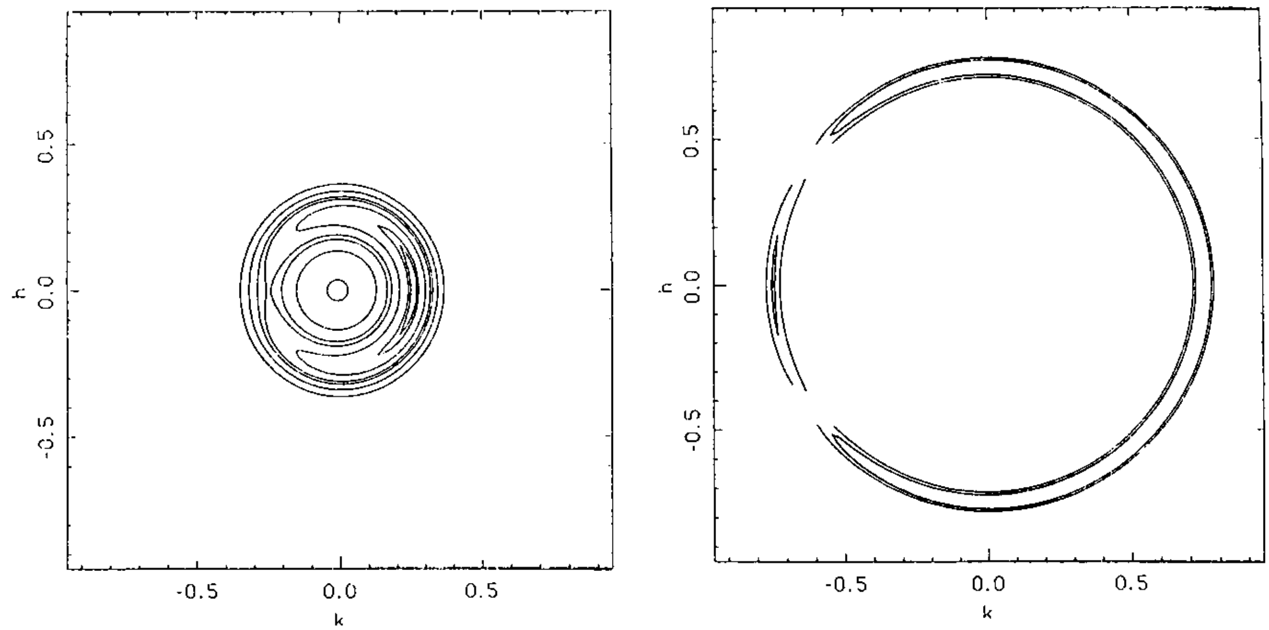

FIG. 1. Typical phase space of $\mathcal{H}_0$, here on the surfaces $N = 0.82$ (left) and $N = 1.04$ (right). The coordinates are $k = e\cos(\sigma)$ and $h = e\sin(\sigma)$.

With this choice of variables, $\mathcal{H}_0$ is reduced to $\mathcal{H}_0(J, J')$ and the unperturbed frequencies of the system are given by

$$\omega_1 = \dot{\psi} = \frac{\partial \mathcal{H}_0}{\partial J} = \frac{2\pi}{T}, \quad \omega_2 = \dot{\psi}' = \frac{\partial \mathcal{H}_0}{\partial J'} = \frac{1}{T}\int_0^T \frac{\partial \mathcal{H}_0}{\partial N}\,dt. \tag{7}$$

On the other hand, with the introduction of the action–angle variables (6) into the perturbation, the total Hamiltonian (4) is transformed into

$$\mathcal{H} = g_5\Lambda_5' + g_6\Lambda_6' + \mathcal{H}_0(J, J') + m_{5,5}\mathcal{H}_{1,5}(\psi, J, \psi', J', \tilde{\omega}_5') + m_{5,6}\mathcal{H}_{1,6}(\psi, J, \psi', J', \tilde{\omega}_6'). \tag{8}$$

Let us now consider the secular resonances introduced by the perturbation; these are given by 1/1 commensurabilities between the mean frequency of the longitude of perihelion of the asteroid and one of the frequencies g_5 and g_6 of Jupiter's longitude of perihelion, i.e., they correspond to $\omega_2 + g_5 = 0$ (for ν_5) and $\omega_2 + g_6 = 0$ (for ν_6). Indeed,

$$\omega_2 = \langle\dot{\nu}\rangle = \langle\dot{\sigma} + \dot{\nu}\rangle = \langle -\dot{\omega}\rangle.$$

These secular resonances can be located in the plane (a, e) by drawing the level curves of $\omega_2 = -g_5$ and $\omega_2 = -g_6$ as functions of the initial conditions of integration $(a, e, \sigma = 0)$. The results are given in Fig. 3 for the 2/1 resonance and in Fig. 10 for the 3/2 one. We see that the two secular resonances are relatively close to each other but, up to now, we have no idea of their real extent. Unfortunately, we are not able to take both of them together into account by an analytical theory. We shall therefore, in a first approximation, consider each of them separately, neglecting the first one when studying the second one, even if we already know that this approach is not realistic as soon as the two resonances overlap or are very close to each other.

Let us neglect, for the moment, the contributions in $\tilde{\omega}_6'$ and consider only the harmonics in $\tilde{\omega}_5'$. We use the canonical variables

$$\begin{array}{ll} \psi, & J \\ \psi_5' = \psi' + \tilde{\omega}_5', & J' \\ \tilde{\omega}_5', & \Pi_5' = \Lambda_5' - J', \end{array} \tag{9}$$

and the resulting Hamiltonian,

$$\mathcal{H} = g_5(\Pi_5' + J') + \mathcal{H}_0(J, J') + m_{5,5}\mathcal{H}_{1,5}(\psi, J, \psi_5', J'), \tag{10}$$

is, in fact, a two-degree-of-freedom one as it is independent of $\tilde{\omega}_5'$, the momentum Π_5' being thus a constant.

This Hamiltonian can be averaged with respect to the angular variable ψ, which, in the region near the ν_5 resonance, is a much faster variable than ψ_5'. This is done by using the seminumerical first-order perturbation method of Henrard (1990) and, in this way, we get an integrable model for the ν_5 secular resonance in the plane,

$$\overline{\mathcal{K}} = g_5\overline{J}' + \overline{\mathcal{K}}_0(\overline{J},\overline{J}') + e'\overline{A}_5(\overline{J},\overline{J}')\cos(\overline{\psi}_5'), \quad (11)$$

with

$$\overline{A}_5(\overline{J},\overline{J}') = \frac{1}{T}\int_0^T \mathcal{H}_{1,5}(\sigma(t), S(t), \nu(t) - \omega_2 t, N(t), \tilde{\omega}_5' = 0)\, dt \quad (12)$$

and where $e' = m_{5,5}$ and $\overline{\psi}_5' = \langle\tilde{\omega}_5' - \tilde{\omega}\rangle$; the integral is computed along the torus (J, J') of $\mathcal{H}_0$ as in Eq. (6).

The action $\overline{J} = J + O(e')$ being an integral of motion, we can plot the level curves of $\overline{\mathcal{K}}$ on given surfaces $J = C'$ in order to see the dynamics in $\overline{\psi}_5' = \tilde{\omega}_5' - \tilde{\omega} + O(e')$. We can also compute the separatrices of Eq. (11) and draw their traces in the plane (a, e, $\sigma = 0$, $\psi_5' = \psi^*$) in order to see the amplitude of the ν_5 resonance, ψ^* being the value of ψ_5' corresponding to the stable equilibrium point of Eq. (11).

Let us recall, however, that we have temporarily neglected the harmonics in $\tilde{\omega}_6'$. Before going further, it is necessary to take them into account. We shall thus do for the ν_6 exactly what we have done for the ν_5 (this one being in its turn neglected), the integral of motion $\overline{J}$ being common to both problems.

The result is astonishing (see Figs. 3 and 10): the two resonances are very broad, the region of overlapping being very wide. An analytical model neglecting their combined effects is thus not realistic.

In order to describe the mutual effects of the ν_5 and ν_6 resonances inside a mean motion resonance $(p + q)/p$ in the frame of the planar problem, we shall now integrate numerically the averaged model obtained by the juxtaposition of the two independent analytical models constructed previously:

$$\overline{\mathcal{K}} = (g_5 + g_6)\overline{J}' + \overline{\mathcal{K}}_0(\overline{J},\overline{J}') + m_{5,5}\overline{A}_5(\overline{J},\overline{J}')\cos(\overline{\psi}_5') + m_{5,6}\overline{A}_6(\overline{J},\overline{J}')\cos(\overline{\psi}_6'). \quad (13)$$

To perform such an integration in a quick way, we compute $\overline{A}_5$, $\overline{A}_6$, $\overline{\mathcal{K}}_0$, and their derivatives on a grid in the $(\overline{J},\overline{J}')$ plane and we interpolate, as in Morbidelli (1992). The results of this integration are presented in Section 3.1 for the 2/1 resonance and in Section 4.1 for the 3/2 one.

2.2 The Three-Dimensional Problem

As we have seen at the beginning of this section, the three-dimensional problem is a six-degree-of-freedom problem containing all the phase space variables (Eq. (3)), except the couple (λ', Λ').

The Hamiltonian of this problem is

$$\mathcal{H} = g_5\Lambda_5' + g_6\Lambda_6' + s_6\Lambda_{16}' + \mathcal{H}_0 + \mathcal{H}_1, \quad (14)$$

where the unperturbed part $\mathcal{H}_0$ can be written

$$\mathcal{H}_0 = \mathcal{H}_{00}(\sigma, S, S_z, N) + \mathcal{H}_{01}(\sigma, S, \sigma_z, S_z, N) \quad (15)$$

and where the perturbation $\mathcal{H}_1$ has the form

$$\mathcal{H}_1 = m_{5,5}\mathcal{H}_{1,5} + m_{5,6}\mathcal{H}_{1,6} + n_{5,6}\mathcal{H}_{1,16}, \quad (16)$$

$\mathcal{H}_{1,5}$ containing the harmonics in $\tilde{\omega}_5'$, $\mathcal{H}_{1,6}$ the harmonics in $\tilde{\omega}_6'$, and $\mathcal{H}_{1,16}$ the harmonics in Ω'.

Let us first introduce action–angle variables for the three-degree-of-freedom separable Hamiltonian $\mathcal{H}_{00}$. We define

$$\begin{aligned} \psi &= \frac{2\pi}{T}t, & J &= \frac{1}{2\pi}\oint S\, d\sigma \\ \psi_z &= \sigma_z - \rho_z(\psi, J, J_z, J'), & J_z &= S_z \\ \psi' &= \nu - \rho'(\psi, J, J_z, J'), & J' &= N. \end{aligned} \quad (17)$$

With this choice of variables, the unperturbed part (Eq. (15)) of the Hamiltonian (Eq. (14)) is reduced to

$$\mathcal{F}_0 = \mathcal{F}_{00}(J, J_z, J') + \mathcal{F}_{01}(\psi, J, \psi_z, J_z, J'). \quad (18)$$

Averaging over ψ, $\mathcal{F}_0$ is transformed into

$$\overline{\mathcal{F}}_0 = \overline{\mathcal{F}}_{00}(\overline{J}, \overline{J}_z, \overline{J}') + \overline{\mathcal{F}}_{01}(\overline{J}, \overline{\psi}_z, \overline{J}_z, \overline{J}'), \quad (19)$$

the action $\overline{J}$ being now a constant as the whole Hamiltonian, including the perturbation, is becoming independent of $\overline{\psi}$. This averaging can be performed in a consistent way provided that there are no relevant secondary resonances between ψ and ψ_z. As a matter of fact, according to Morbidelli and Giorgilli (1990) $\dot{\psi}$ is 10 times larger than $\dot{\psi}_z$ at $e \sim 0.2$ in both 2/1 and 3/2, so that such secondary resonances should not be predominant in the region of not small eccentricity where secular resonances will be located.

With little loss of generality, we may restrict our study to the limiting case $\overline{J} \rightarrow 0$, which corresponds to the family of stable equilibrium points (pericentric branch) of the first degree of freedom. In this case, the periodic functions ρ and ρ_z vanish, and the variables $(\overline{J}, \overline{\psi}_z, \overline{J}_z, \overline{\psi}', \overline{J}')$ are exactly $(J, \sigma_z, S_z, \nu, N)$ when evaluated along the pericentric branch. For the sake of simplicity, we shall assume that, from now on, each quantity refers to its value along this branch, avoiding the introduction of new notations;

for instance, $\sigma_z = \omega$ and $\nu = -\tilde{\omega}$, whereas the semimajor axis becomes a function of e and i. The integrable part (Eq. (19)) of the Hamiltonian reads then $\overline{\mathcal{F}}_0(\omega, S_z, N)$.

The dynamics of $\overline{\mathcal{F}}_0(\omega, S_z, N)$ is dominated by the term in $i^2 \cos 2\omega$. Three typical phase space portraits of it are given in Fig. 5 (see Section 3.2 for comments) for three different values of N. A global view, taking into account the variations of N, is given in the plane $(e, i, \omega = \pi/2)$ in Figs. 6 and 13, the leftmost zones of which correspond to $\dot{\omega} < 0$ *and the rightmost zones to* $\dot{\omega} > 0$.

Let us introduce action–angle variables for the two-degree-of-freedom separable Hamiltonian $\overline{\mathcal{F}}_0(\omega, S_z, N)$. We define

$$\psi_\omega = \frac{2\pi}{T_\omega} t, \qquad J_\omega = \frac{1}{2\pi} \oint S_z \, d\omega$$
$$\omega' = \nu - \rho(\psi_\omega, J_\omega, J'), \quad J' = N, \tag{20}$$

where the integral is now computed along a given torus of $\overline{\mathcal{F}}_0(\omega, S_z, N)$, T_ω being the period on the torus.

The integrable part $\overline{\mathcal{F}}_0(\omega, S_z, N)$ of the Hamiltonian (Eq. (14)) becomes now $\mathcal{H}_0(J_\omega, J')$ and the unperturbed frequencies are

$$\omega_1 = \dot{\psi}_\omega = \frac{\partial \mathcal{H}_0}{\partial J_\omega} = \frac{2\pi}{T_\omega},$$
$$\omega_2 = \dot{\psi}' = \frac{\partial \mathcal{H}_0}{\partial J'} = \frac{1}{T_\omega} \int_0^{T_\omega} \frac{\partial \overline{\mathcal{F}}_0}{\partial N} dt. \tag{21}$$

On the other hand, with the introduction of the action–angle variables (20) into the perturbation, the total Hamiltonian (Eq. (14)) is transformed into

$$\begin{aligned} \mathcal{H} = {} & g_5 \Lambda_5' + g_6 \Lambda_6' + s_6 \Lambda_{16}' + \mathcal{H}_0(J_\omega, J') \\ & + n_{5,6} \mathcal{H}_{1,16}(\psi_\omega, J_\omega, \psi', J', \Omega') \\ & + m_{5,5} \mathcal{H}_{1,5}(\psi_\omega, J_\omega, \psi', J', \tilde{\omega}_5') \\ & + m_{5,6} \mathcal{H}_{1,6}(\psi_\omega, J_\omega, \psi', J', \tilde{\omega}_6'). \end{aligned} \tag{22}$$

Let us now consider the secular resonances introduced by the perturbation; these are given by 1/1 commensurabilities between the mean frequency of the longitude of perihelion of the asteroid and one of the frequencies g_5 and g_6 of Jupiter's longitude of perihelion and also by the 1/1 commensurability between the mean frequency of the longitude of the node of the asteroid and the frequency s_6 of Jupiter's longitude of node. They correspond thus to $\omega_2 + g_5 = 0$ (for ν_5), $\omega_2 + g_6 = 0$ (for ν_6), and $\langle\dot{\omega}\rangle + \omega_2 + s_6 = 0$ (for ν_{16}), where $\langle\dot{\omega}\rangle$ is equal to ω_1 (resp. $-\omega_1$) in the region of positive (resp. negative) circulation of ω, its value being 0 in the libration zone.

These secular resonances can be located in the plane (e, i) by drawing the level curves of $\omega_2 = -g_5$, $\omega_2 = -g_6$, and $\langle\dot{\omega}\rangle + \omega_2 = -s_6$ as functions of the initial conditions of integration $(e, i, \omega = \pi/2)$. The results for the 2/1 resonance are given in Fig. 7 and for the 3/2 one in Fig. 14. In these figures, we have only plotted the ν_{16} resonance, which stays in the region of negative circulation of ω. The secular resonances ν_5 and ν_6 are not plotted: they are very near the ω-separatrix, in the region of positive circulation of ω.

In order to describe the ν_{16} resonance, we shall now *restrict our study to the region of negative circulation of* ω. In this region, the effect of the harmonics in $\tilde{\omega}_5'$ and $\tilde{\omega}_6'$ is negligible and the Hamiltonian (Eq. (22)) is reduced to

$$\mathcal{H} = s_6 \Lambda_{16}' + \mathcal{H}_0(J_\omega, J') + n_{5,6} \mathcal{H}_{1,16}(\psi_\omega, J_\omega, \psi', J', \Omega'). \tag{23}$$

As in the planar case, we introduce canonical variables appropriate to the secular resonance involved. These are

$$\begin{aligned} &\psi_\omega, && J_\omega' = J_\omega + J' \\ &\psi_{16}' = \psi' - \psi_\omega + \Omega', && J' \\ &\Omega', && \Pi_{16}' = \Lambda_{16}' - J' \end{aligned} \tag{24}$$

and transform the Hamiltonian (Eq. (23)) into

$$\mathcal{H} = s_6(\Pi_{16}' + J') + \mathcal{H}_0(J_\omega', J') + n_{5,6} \mathcal{H}_{1,16}(\psi_\omega, J_\omega', \psi_{16}', J'). \tag{25}$$

The two-degree-of-freedom Hamiltonian (Eq. (25)) is finally averaged with respect to ψ_ω, which, in the region of the phase space near the ν_{16} resonance, is a much faster variable than ψ_{16}'. This provides us with the integrable Hamiltonian for the ν_{16} resonance,

$$\overline{\mathcal{H}} = s_6 \overline{J}' + \mathcal{H}_0(\overline{J}_\omega', \overline{J}') + i' \overline{A}_{16}(\overline{J}_\omega', \overline{J}') \cos(\overline{\psi}_{16}'), \tag{26}$$

with

$$\overline{A}_{16}(\overline{J}_\omega', \overline{J}') = \frac{1}{T_\omega} \int_0^{T_\omega} \mathcal{F}_{1,16}(\omega(t), S_z(t), \nu(t) + (\omega_1 - \omega_2)t, N(t), \Omega' = 0)\, dt \tag{27}$$

and where $i' = n_{5,6}$ and $\psi_{16}' = \langle\Omega' - \Omega\rangle$; the integral is computed along the torus (J_ω, J') of $\overline{\mathcal{F}}_0$ as in Eq. (20).

The action $\overline{J}_\omega' = J_\omega' + O(i')$ is now an integral of motion, and, for each value of J_ω', we can compute the location of the separatrices of Eq. (26) and draw their traces in the plane $(e, i, \omega = \pi/2, \psi_{16}' = \psi^*)$ in order to see the amplitude of the ν_{16} resonance, ψ^* being the value of ψ_{16}' corresponding to the stable equilibrium point of Eq. (26).

The results are presented in Section 3.2 for the 2/1 resonance and in Section 4.2 for the 3/2 one.

3. THE 2/1 MEAN MOTION COMMENSURABILITY

This section is devoted to the description of the dynamics in the 2/1 mean motion resonance. First we analyze the dynamics on the plane, assuming the inclinations of all the planets to be zero. Later, we shall take into account the inclination of Jupiter's orbit over the reference plane and the precession of its longitude of node; this leads us to investigate the dynamics in three dimensions.

3.1. Motion on the Plane

In first approximation, we assume the orbit of Jupiter to be circular, therefore assuming the eccentricity of Jupiter as a perturbation parameter. From the physical point of view, this is justified by the fact that the motion described by the circular problem is the one with the shortest timescale.

After averaging over the mean longitude of Jupiter (λ'), the *planar* circular problem is integrable. For a complete discussion of this problem, taking into account also the collisions with Jupiter and the bifurcations of families of equilibrium points (which are the periodic orbits of the nonaveraged problem), we refer to Moons and Morbidelli (1992). For our purposes here it is sufficient to recall that the dynamics described by the averaged circular problem (also outside of the plane) has a constant of motion

$$N = \sqrt{(1-\mu)a}(2 - \sqrt{1-e^2}\cos i), \qquad (28)$$

where a, e, and i are the semimajor axis, the eccentricity, and the inclination of the asteroid, respectively. On the reference plane $i = 0$ the curves N equal constant have the shape plotted in Fig. 2. In the same picture the solid line denotes the main stable family of equilibrium points, usually called the *pericentric branch*. The two thick lines on the sides of the picture denote the separatrices, which can be considered as the real bounds of the mean motion resonance. Indeed the critical angle of the resonance, here

$$\sigma = 2\lambda' - \lambda - \tilde{\omega}$$

(λ and $\tilde{\omega}$ being the mean longitude and the longitude of perihelion of the asteroid) librates for all orbits with initial conditions at $\sigma = 0$ between the two thick lines. For these orbits, a and e oscillate, together with the libration of σ, on a line N = constant, passing from the left side to the right side of the stable branch and vice versa. The maximal distance from the stable branch is reached when $\sigma = 0$ ($\dot{\sigma} < 0$ on the left side and $\dot{\sigma} > 0$ on the right side).

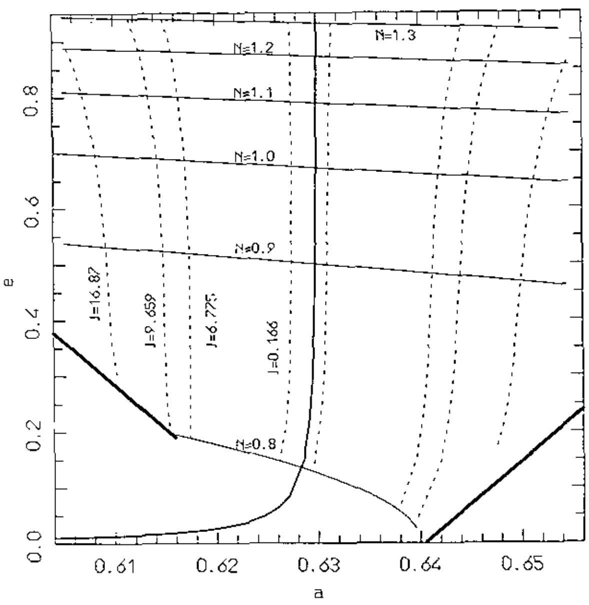

FIG. 2. Dynamics in the 2/1 commensurability: the central bold curve is the stable family of periodic orbits of the planar circular restricted problem; the two thick lines on the sides denote the separatrices at $\sigma = 0$: the solid lines mark some levels N = constant and the dashed lines denote some level J = constant (all J values multiplied by 10^{-3}). The semimajor axis unit is a'.

Therefore, the separatrices denote the maximal libration amplitude.

The separatices disappear for $N \lesssim 0.8$. In some sense we are no longer in presence of a *resonance*. We skip the study of this region, since it has been already investigated in detail by means of truncated models, as in Lemaître and Henrard (1990). Moreover, in a previous paper (Moons and Morbidelli 1992) we have studied extensively this region by computing numerically Poincaré sections of the averaged planar elliptic three-body problem. Conversely, at large eccentricity, we limit our study to librating orbits in the interval $0.604 < a < 0.656$: indeed these orbits avoid collisions with Jupiter, being deeply inside the mean motion resonance (see Moons and Morbidelli 1992).

We come now to analyze the effects produced by the eccentricity of Jupiter's orbit.

The main effect is that the action N is no longer a constant of motion. N changes on a longer timescale (at least 10 times longer than the period of libration of σ) together with the motion of the asteroid's longitude of perihelion and with time (since Jupiter's eccentricity and perihelion change with time). However, the area J enclosed by the trajectory during the σ-libration (rigorously defined in Section 2) is an adiabatic invariant. In Fig. 2 the dashed lines denote a few curves J = constant on the (a, e) plane at $\sigma = 0$. This picture should be interpreted

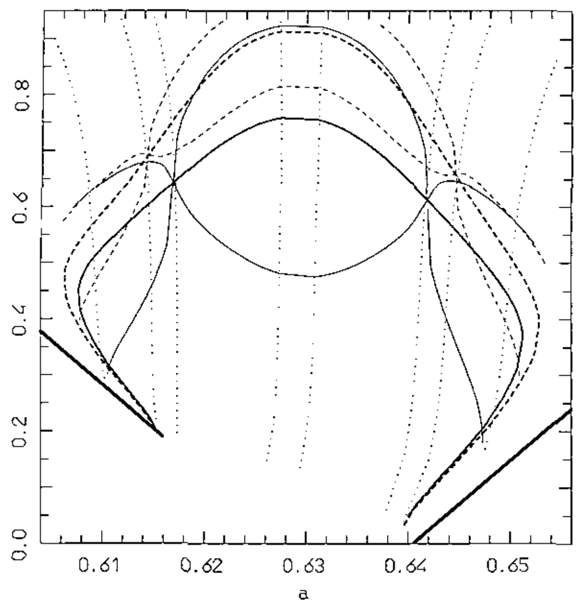

FIG. 3. Secular resonances in the 2/1 commensurability on the plane $i = 0$: the solid bold line marks the location of the ν_5 resonance, the dashed bold line the location of the ν_6; the two thin solid lines and the two thin dashed lines denote the separatrices of ν_5 and ν_6 respectively; the dotted lines are the J levels on which numerical integrations of the two-resonance secular system are performed.

as follows: the dynamics change slowly, changing the value of N, but in such a way that any time $\sigma = 0$, a and e are always on the same dashed line.

The variation of N can have different behaviors, (small, large, regular, or chaotic) in the different regions of the space. In particular, relevant phenomena can occur near the two secular resonances ν_5 and ν_6. In Fig. 3 we report the location of these two resonances, the bold solid line denoting the ν_5 and the bold dashed line the ν_6. Moreover the couple of solid lines (for ν_5) and the couple of dashed lines (for ν_6) delimit the amplitudes of the two secular resonances. These are computed by taking into account only one resonance at a time, namely neglecting all mutual interactions, and are defined by the location of the corresponding separatrices (see Section 2 for a detailed description of the procedure).

As one sees, both resonances shrink for some given value of the action J (the dotted lines denoting the same J curves as in Fig. 2). This is due to the fact that the topology of the resonances changes: the stable and the unstable equilibrium points exchange their position, and in this transition the amplitude of the resonance goes to zero. This is the picture one gets, of course, neglecting mutual interactions between the resonances, and this is a crude approximation, since the two resonances overlap. In particular, one can expect a lot of chaos to be generated by this overlapping.

The best way to study the interaction between the two secular resonances is to integrate numerically the secular system on different surfaces J = constant (see Section 2 for the details). In Fig. 4 we report our results concerning the four values of J indicated in Figs. 2 and 3.

Each picture of Fig. 4 is a surface of section of the secular system. The coordinates reported on the axes are N and $q = \tilde{\omega} - g_5 t$, the latter being the critical angle of the ν_5 secular resonance. The section is made on the critical angle of the ν_6 resonance, namely $q' = \tilde{\omega} - g_6 t$ (0 or π depending on the J-level in study). It is worth noting that, g_5 being the average frequency of Jupiter's longitude of perihelion $\tilde{\omega}_J$ and g_6 the average frequency of Saturn's longitude of perihelion $\tilde{\omega}_S$, the critical angles q and q' are usually indicated in the literature as $\tilde{\omega} - \omega_J$ and $\tilde{\omega} - \tilde{\omega}_S$, respectively.

We stress that our surfaces of section are not transversal to the dynamics; namely, they are not Poincaré sections. This is due to the fact that the angle q' may circulate in both directions or librate. However they are very useful in distinguishing chaotic motion from a quasi-integrable one. The lines N = constant and J = constant of Fig. 2 allow translation of the results into the original variables a and e.

The first picture of Fig. 4 has been computed for $J = 0.166 \times 10^{-3}$. The section is made at $q' = \pi$. The chaotic region dominates for $N \gtrsim 0.88$ ($e \gtrsim 0.45$); only a small island of regular motion exists at $N = 0.98$, $q = 0$. This is the core of the ν_5 secular resonance. Chaotic orbits may escape from the Solar System, the action N exceeding 1.3, i.e., the eccentricity becoming larger than 1. Regular trajectories (i.e., invariant tori) with circulation of q exist only at moderate eccentricities.

The second picture of Fig. 4 has been computed for $J = 6.775 \times 10^{-3}$. The section is made at $q' = \pi$. Such a value of J corresponds to the change of topology in the ν_5 resonance, as one can see in Fig. 3. The numerical integration shows two small regular islands at $q = 0$ and $q = \pi$. The two islands are independent, each one corresponding to a different orbit. This is what is left of the ν_5 resonance while it shrinks. The chaotic region is very small, since the ν_5 resonance is almost nonexistent. The two pairs of regular tori which cross the axis $q = 0$ between $N = 1.08$ and $N = 1.1$ are the trace of an island of regular motion of the ν_6 resonance, where $q' = \tilde{\omega} - g_6 t$ librates. Regular trajectories exist for $N \lesssim 0.97$ and $N \gtrsim 1.15$ at $q = 0$.

The third picture of Fig. 4 has been computed for $J = 9.659 \times 10^{-3}$. The section is made at $q' = \pi$. Now it is the ν_6 resonance which shrinks, changing topology; therefore the chaotic layer is again small. A wide regular island exist at $q = \pi$, which is the libration region of the ν_5 resonance.

Finally, the last picture of Fig. 4 has been computed

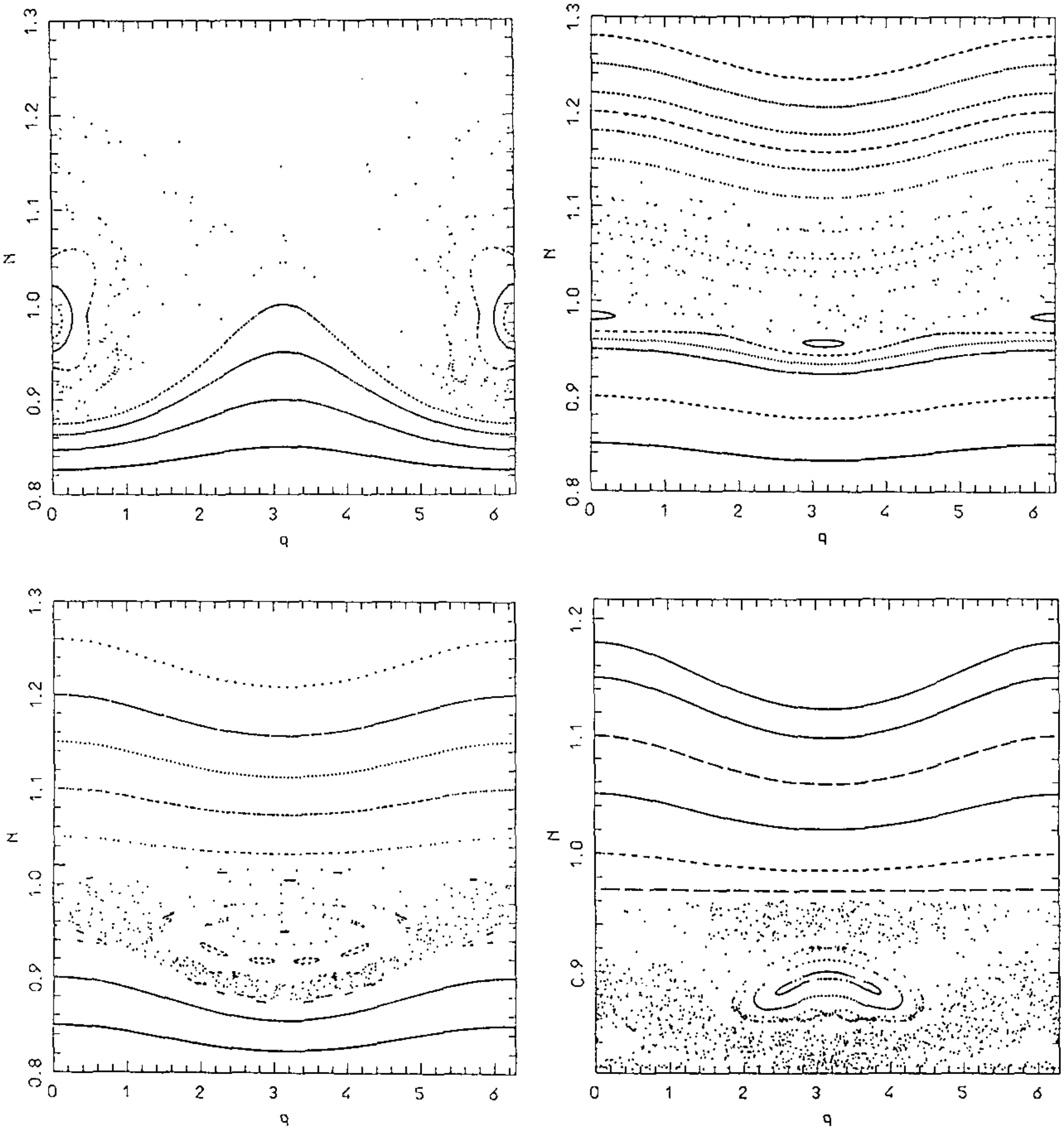

FIG. 4. Numerical integrations of the secular system $\nu_5 + \nu_6$. Top left, $J = 0.166 \times 10^{-3}$. Top right, $J = 6.775 \times 10^{-3}$. Bottom left, $J = 9.659 \times 10^{-3}$. Bottom right, $J = 16.87 \times 10^{-3}$. See text for comments.

for $J = 16.87 \times 10^{-3}$. The section is made at $q' = 0$. The interaction between the two secular resonances is very strong again: the chaotic layer is large, and only a small island of regular motion exists at $q = \pi$. Invariant tori with circulating q exist only for $N \gtrsim 0.97$ (i.e., $e \gtrsim 0.6$).

In conclusion, we point out that the interaction between the two secular resonances is very important and gives origin to wide chaotic layers where islands are small. This result is completely different with respect to the one obtained in the framework of the restricted three body problem (see Yoshikawa 1989), where only one secular resonance is present in the model. However, orbits with small J (i.e., small amplitude of libration in σ) and moderate eccentricity turn out to be regular, at this stage.

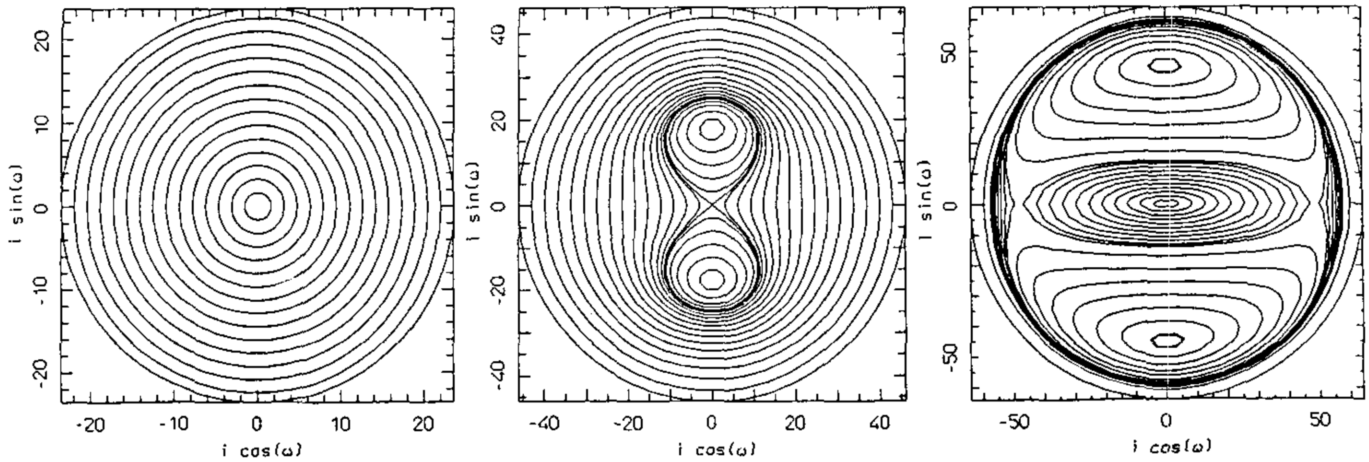

FIG. 5. Typical phase-portrait of the dynamics of the argument of perihelion, in polar coordinates (i, ω). The picture on the left concerns a N-level which does not intersect the resonance; the picture in the center concerns a N-level which intersects only the stable family; the picture on the right is for a N-level which cuts both stable and unstable families.

3.2. Motion Outside of the Plane

Even in the framework of the restricted circular three body problem ($e' = 0$), the averaged Hamiltonian describing a mean motion resonance at nonzero inclination is nonintegrable, since it depends on two angles, namely the critical angle σ and the argument of perihelion ω. A perturbation approach is necessary in order to explore the dynamics, finding out an integrable approximation. This is what we do by successive elimination of harmonics (see Section 2). Here we show the results obtained for orbits with small amplitude of libration in σ, namely in the limit $J \to 0$. This is done for simplicity, in order to be able to represent the dynamics on a two-dimensional plane with coordinates e and i; the semimajor axis can be eliminated in this way, since we are working along the pericentric branch.

In Fig. 6 the dotted curves denote the levels $N =$ constant, with N given by Eq. (28). Eccentricity and inclination evolve on these lines as a consequence of the motion of the argument of perihelion ω.

The motion of ω is not a simple one. A resonance occurs at large eccentricity. A typical portrait of the dynamics is that shown in Fig. 5. Stable and unstable equilibrium points form families parametrized by the value of N. In Fig. 6 the solid line denotes the family of stable equilibrium points, where the argument of perihelion ω is fixed at $\pi/2$ or $3\pi/2$; the dashed line denotes the unstable family of equilibrium points, with $\omega = 0$ or $\omega = \pi$; the two thick lines mark the position of the separatrices at $\omega = \pi/2$, $3\pi/2$. The argument of perihelion circulates with negative derivative for any initial condition on the left side of the leftmost separatrix and circulates with positive derivative on the right side of the rightmost one. Conversely, any orbit with initial conditions between the two separatrices at $\omega = \pi/2$ or $\omega = 3\pi/2$ librates around the stable family. The location of the families of periodic orbits has been found first by Morbidelli and Giorgilli (1990), and we confirm here that result, providing also a global description of the dynamics.

We come now to the effects produced by Jupiter's eccentricity and inclination and their time-dependent variations. We restrict our analysis to the region of negative circulation of ω, in particular in the region with $e < 0.4$. In this region, neither the ν_5 nor the ν_6 secular resonances are present; indeed both can be found only in the region of positive ω-circulation, near the ω-separatrix. Therefore their effects are not very relevant, as it already happened on the plane at small eccentricity.

Much more relevant is the effect of Jupiter's inclination and of the precession of its longitude of node. This causes the slow variation of N, the action J'_ω being an adiabatic invariant (see Section 2). In Fig. 7 the dotted lines denote some levels $J'_\omega =$ constant. Again the picture must be interpreted in the following way: the dynamics change slowly, changing the value of N, but in such a way that, any time $\omega = \pi/2$, e and i are always on the same dotted line.

Like in the planar case, the variations of N are relevant close to a secular resonance. In Fig. 7 the bold dashed line denotes the location of the ν_{16} secular resonance, which is the corotation of the longitudes of the node of the asteroid and of Jupiter, denoted by Ω and Ω_J, respectively. The result is astonishing: the resonance cuts the plane $i = 0$ at moderate eccentricity, namely $e = 0.21$; therefore it would cross a family of fictitious asteroids with the same distribution of e and i like that of the Hildas.

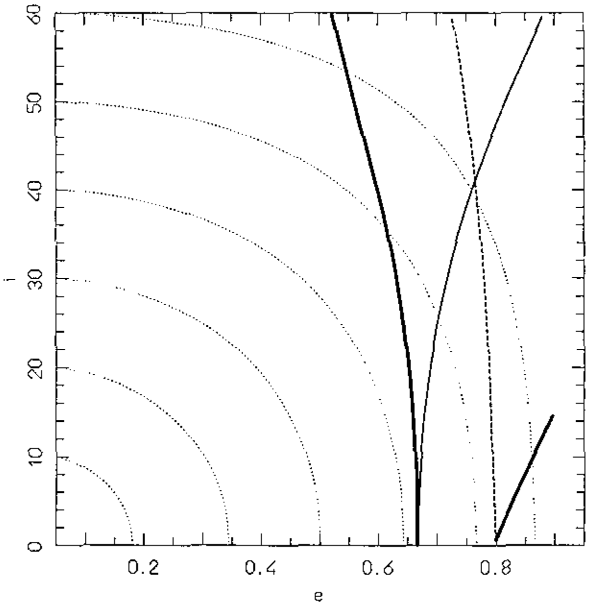

FIG. 6. Dynamics outside of the reference plane, in the restricted circular three-body problem: the solid curve is the stable family of equilibrium points of the argument of perihelion ($\omega = \pi/2, 3\pi/2$); the dashed line is the unstable one ($\omega = 0, \pi$); the two thick lines denote the separatrices of the region of ω-libration at $\omega = \pi/2$; the dotted curves are levels N = constant.

Is this enough to explain the puzzling existence of the Hecuba gap?

Unfortunately, this is not the case, apparently. The ν_{16} resonance seems isolated from the resonance of the argument of perihelion and from other secular resonances of low order. This allows us to construct easily an integrable model to describe its dynamics, using the technique of successive elimination of harmonics (see Section 2). In this way we can compute the amplitude of the resonance (denoted by the two dashed lines in Fig. 7) given by the location of the separatrices of this integrable model and determine that the banana-shaped libration of the critical angle of the secular resonance, namely $\Omega - \Omega_J$, is always around π. However, even if this can explain periodic excursions to the region at high inclination, it does not explain why the asteroids should be absent. Indeed, there is no clear mechanism for the depletion of asteroids at large inclination; on the other hand, looking at the lines J'_ω = constant, we can predict that during the variation of the inclination, the eccentricity should be bounded to moderate values.

We have performed a few numerical integrations of fictitious asteroids in order to confirm our previsions on the existence and on the dynamics of the ν_{16} resonance. These have been made by using the Everhart's numerical integrator RA15 and integrating the full equations of motion of the Sun–asteroid–Jupiter–Saturn system. No simplifications have been introduced in this model (apart having neglected the other planets of the Solar System). Figure 8 shows one of our results. The picture on the left in Fig. 8 shows the evolution of the asteroid orbit in polar coordinates i, $\Omega - \Omega_J$. The arrows indicate the direction of the motion. The first part of the orbit is evidently a banana-shaped libration around $\Omega - \Omega_J = \pi$; afterwards a transition occurs to the outer region where $\Omega - \Omega_J$ circulates counterclockwise. As a consequence, the inclination passes from 10° to 24°.

This numerical simulation proves the existence of the ν_{16} secular resonance in the 2/1 mean motion commensurability; it is in good agreement with the theoretical computations of the location and on the amplitude of the resonance. As matter of fact, the numerical simulation shows that the resonance should be shifted to somewhat larger eccentricity with respect to the position computed in Fig. 8 ($\Delta e \sim 0.03$). This should be due to the fact that our orbit has a nonnegligible amplitude of libration in σ of about 40°. Indeed, we have verified that the secular resonance is shifted to larger e, with increasing J.

The picture on the right in Fig. 8 shows the evolution of the eccentricity over the 1.5-Myr integration. As one sees, it does not increase significantly and never reaches dangerous values for the asteroid's life. Indeed, the ν_{16} secular resonance acts on the inclination and not on the eccentricity. At this stage, therefore, we are not able to explain, by the ν_{16} mechanism, the existence of the Hecuba gap. Longer and more sophisticated numerical integrations should be necessary in order to explore whether

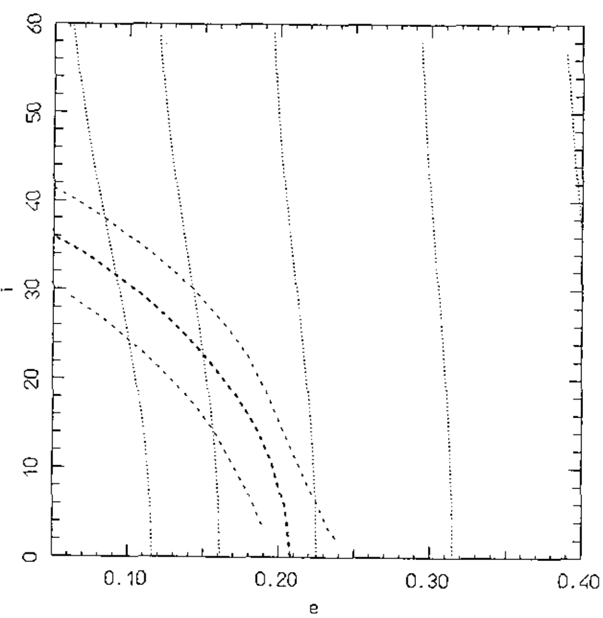

FIG. 7. The location of the ν_{16} secular resonance (bold dashed line) and its separatrices (thin dashed lines). The dotted curves denote some levels J'_ω = constant.

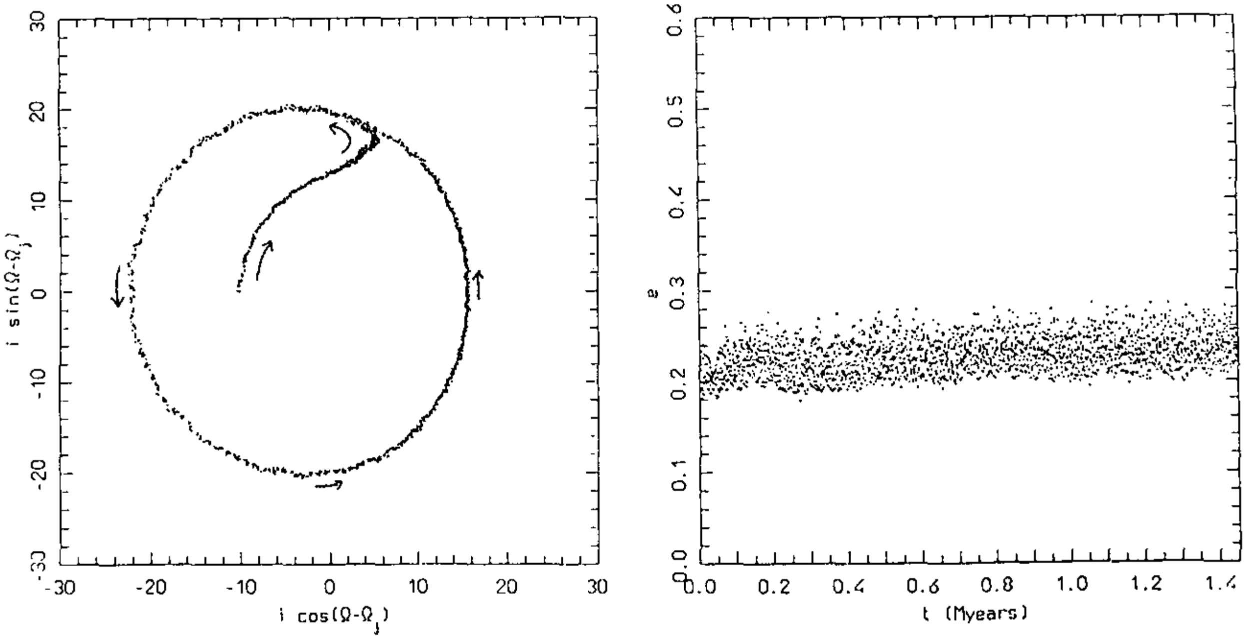

FIG. 8. A numerical simulation of a fictitious asteroid in the ν_{16} resonance: on the left a picture on the evolution of i and $\Omega - \Omega_J$; on the right the evolution of e vs time. Initial conditions are (with respect to the Sun) Asteroid: $\omega = 0.0$, $\Omega = 381.01575$, $i = 10.0$, $e = 0.2$, $a = 3.27278475$, $l = 205.0485$; Jupiter: $\omega_J = 68.21540$, $\Omega_J = 201.01575$, $i_J = 0.36118$, $e_J = 0.04819$, $a_J = 5.20315540$, $l_J = 34.36331$; Saturn: $\omega_S = 324.39864$, $\Omega_S = 21.01575$, $i_S = 0.89097$, $e_S = 0.05469$, $a_S = 9.52355280$, $l_S = 179.52366$. The angles are given in degrees.

at large inclination a sort of diffusion to large eccentricity is possible, jumping from one high-order secondary resonance to another, on a very long timescale. Moreover, the region with small eccentricity and small inclination ($e \lesssim 0.2$, $i \lesssim 10°$) seems to be protected from the ν_{16} resonance. As a matter of fact one real asteroid exists in that region; called 3789 Zhongguo, it has actually the following osculating elements: $a = 3.272181$, $e = 0.1955$, $i = 2.75441$, and $\sigma \sim -61.12°$. It would be interesting to have a long-time numerical simulation, in the past and in the future, of this object.

4. THE 3/2 MEAN MOTION COMMENSURABILITY

In this section we describe the dynamics in the 3/2 mean motion resonance; we follow the same approach adopted for the exploration of the 2/1, in order to point out in a better light their similarities and differences. Again, we start by analyzing the motion on the reference plane, assuming the inclination of the planets equal to zero. Later, we study the dynamics in three dimensions, taking into account Jupiter's inclination and the precession of its node.

4.1. Motion on the Plane

In the case of the 3/2 mean motion commensurability, the critical angle of the resonance σ is

$$\sigma = 3\lambda' - 2\lambda - \tilde{\omega},$$

whereas the constant of motion N of the averaged restricted circular three-body problem is now

$$N = \sqrt{(1-\mu)a}\left(\tfrac{3}{2} - \sqrt{1-e^2}\cos i\right). \qquad (29)$$

In Fig. 9, we report some curves N = constant on the plane $i = 0$. The bold solid line denotes the main stable family of equilibrium points of the averaged planar circular problem, i.e., the *pericentric branch*. The two thick lines on the sides of the picture denote the separatrices. As in Section 3, their positions have been plotted for $\sigma = 0$.

The eccentricity of Jupiter's orbit forces N to change. As in the case of the 2/1 commensurability, this is an adiabatic process, in the sense that the area J enclosed by the trajectory during the σ-libration is preserved. The dashed lines in Fig. 9 denote some levels J = constant in the (a, e) plane at $\sigma = 0$.

In Fig. 10 we plot the location of the secular resonances ν_5 (bold solid line) and ν_6 (bold dashed line); their amplitudes, computed by considering each resonance as an isolated one, and neglecting mutual influences, are indicated by the two solid lines (ν_5) and dashed lines (ν_6). The crosses denote the osculating values of a and e for the asteroids in the Hilda group.

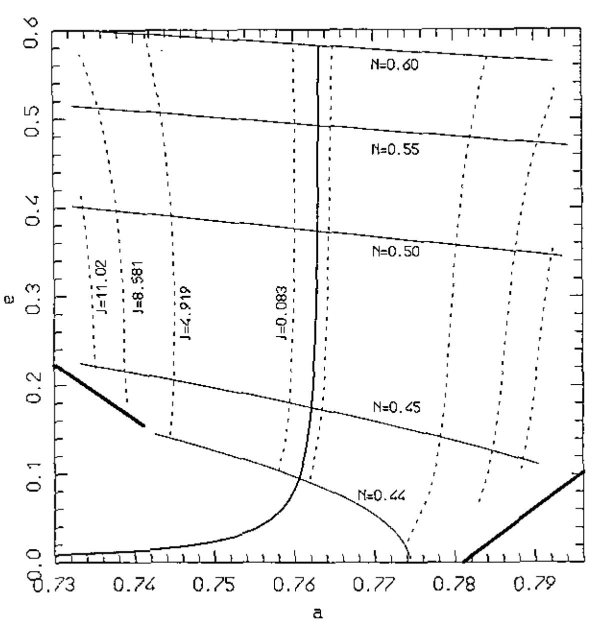

FIG. 9. Dynamics in the 3/2 commensurability: the same as in Fig. 2.

A few differences with respect to the case of the 2/1 commensurability must be emphasized:

- both secular resonances occur at smaller eccentricity, the lowest separatrix of the ν_5 reaching $e = 0.25$;
- neither the ν_5 nor the ν_6 shrinks for some value of J; namely, the two secular resonances do not change their topology;
- the ν_5 and the ν_6 resonances look much closer each other; the overlapping is complete, the ν_6 being "inside" the ν_5.

As in Section 3, we have performed numerical integrations of the secular system on the four J levels denoted by dotted lines in Fig. 10 (the same as in Fig. 9); this is done in order to take into account both secular resonances together and verify the effects of their interaction.

The results are illustrated in Fig. 11: the coordinates of each picture are N and $q = \tilde{\omega} - g_5 t$ and the section of the motion is computed at $q' = \tilde{\omega} - g_6 t = 0$. The N levels and J levels in Fig. 9 allow the translation of the results in the original variables a and e.

The first picture is made for $J = 0.083 \times 10^{-3}$. Regular motion is possible only for $N \lesssim 0.452$ (approximately $e < 0.25$) at $q = \pi$. A big chaotic region exists for $N \gtrsim 0.454$ and $q = \pi$, where only three regular islands are visible. We stress that these islands do not correspond to a 3 : 1 resonance as in the case of a classical Poincaré section; we note also that the island above does not have the same volume as the two ones below. This is precisely due to the fact that our section is not transversal to the motion, since the dynamics of q' is complicated. In Fig. 12 we show the stable periodic orbit which is in the center of the three islands. The picture on the left of Fig. 12 shows the periodic orbit in the variables (q, N); the picture on the right shows the same periodic orbit in the variables (q', N). On a section at $q' = \pi$ this gives three distinct dots on the (q, N) plane.

The second picture is computed for $J = 4.919 \times 10^{-3}$. A relevant island of regular motion is visible in the middle of a wide chaotic layer. Regular motion with circulating q is possible only at large and small N (i.e., $e \lesssim 0.2$ and $e \gtrsim 0.45$).

A similar scenario is visible in the third and the fourth pictures. In the fourth one ($J = 11.02 \times 10^{-3}$), a relevant island of regular motion is visible also at $q = 0$. This is due to the fact that, as illustrated in Fig. 10, the J level in study cuts twice the location of the secular resonance.

The conclusion is similar to that for the 2/1 mean motion commensurability: interaction between secular resonances gives origin to a wide chaotic layer. However, regular motion is possible at moderate eccentricity. It is curious to notice that such a regular region is smaller in the 3/2 commensurability ($e < 0.25$ at $q = \pi$) than in the 2/1 ($e < 0.45$ at $q = 0$). Nevertheless, the 3/2 hosts the asteroids of the Hilda family. These asteroids avoid the ν_5 resonance and its associated chaotic layer, since they are phase protected, as shown

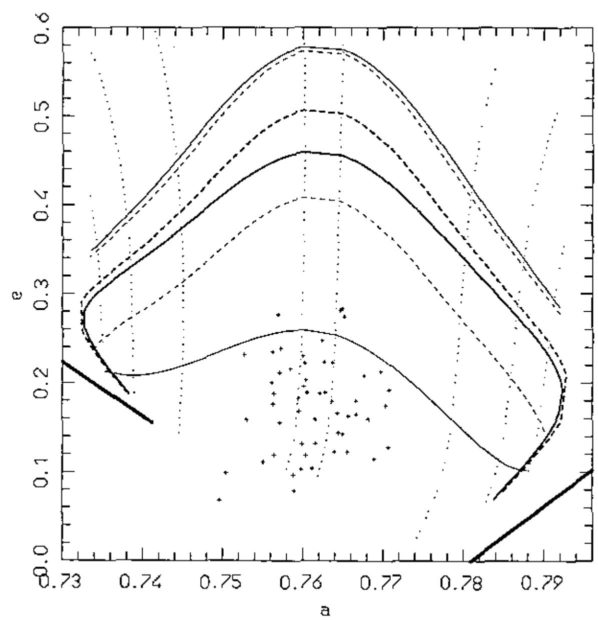

FIG. 10. Secular resonances ν_5 and ν_6 and their separatrices in solid lines and dashed lines respectively. The crosses denote the asteroids of the Hilda group (osculating values). The asteroids which seem to appear inside the ν_5 secular resonance are in fact phase-protected as explained at the end of the section 4.1.

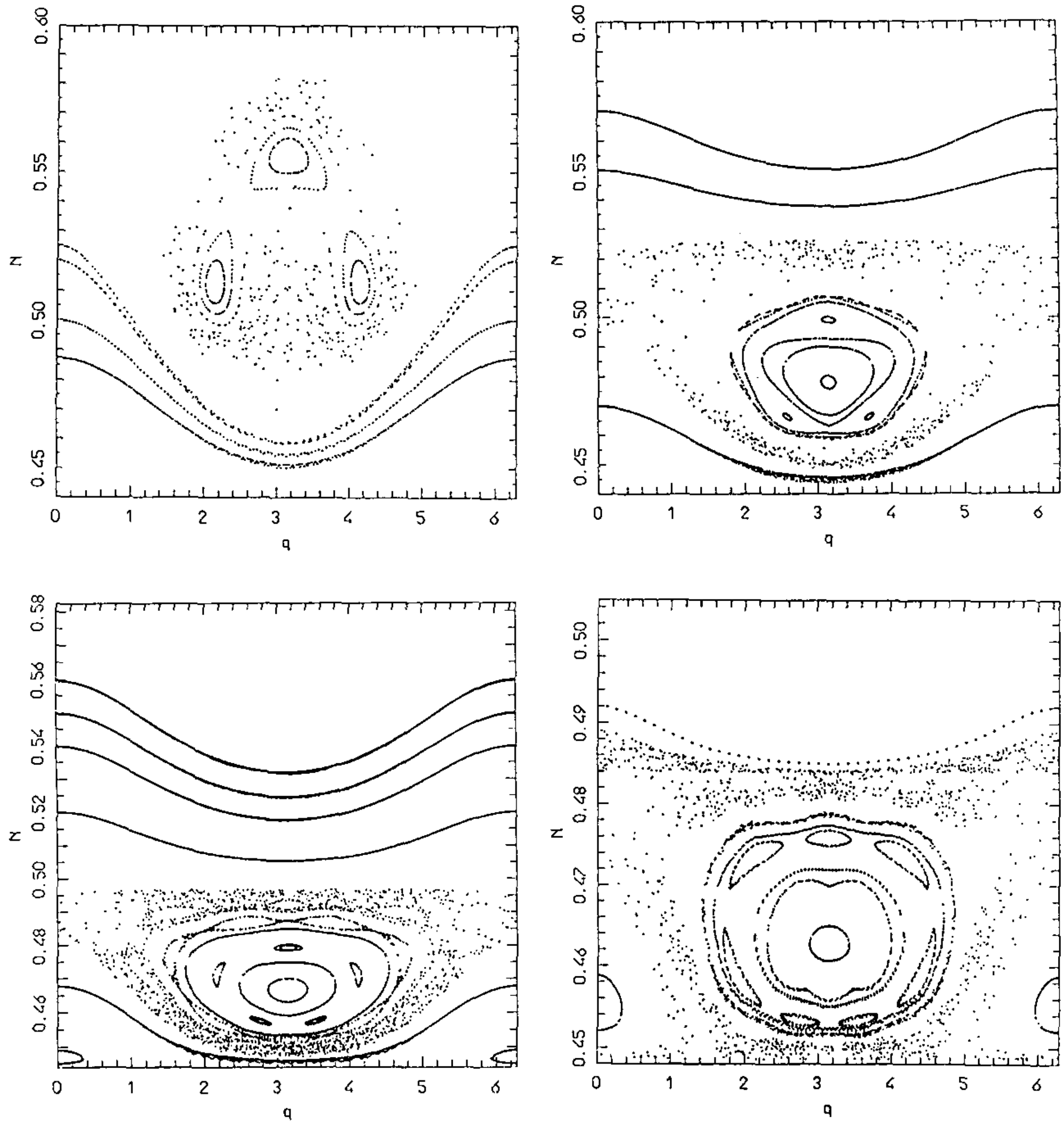

FIG. 11. Numerical integration of the $\nu_5 + \nu_6$ secular system. Top left: $J = 0.083 \times 10^{-3}$. Top right: $J = 4.919 \times 10^{-3}$. Bottom left: $J = 8.581 \times 10^{-3}$. Bottom right: $J = 11.02 \times 10^{-3}$. See text for comments.

by Ferraz-Mello (1988), Morbidelli and Giorgilli (1990), and Michtchenko and Ferraz-Mello (1992); indeed, the Hildas with an eccentricity larger than 0.25 (and which therefore appear in Fig. 10 inside the ν_5 resonance) have a critical angle q close to zero so that they avoid the chaotic layer. As a matter of fact, the chaotic layer is present at $q = 0$ only at $e \gtrsim 0.4$, as one can see in the first picture of Fig. 11.

4.2. Motion Outside of the Plane

As in the case of the 2/1 mean motion commensurability, we restrict our analysis to orbits with small amplitude of σ-libration, since all computations are performed in the limit $J \rightarrow 0$.

Figure 13 shows by dotted lines some levels N = constant on the e, i plane, the eccentricity ranging from 0.05

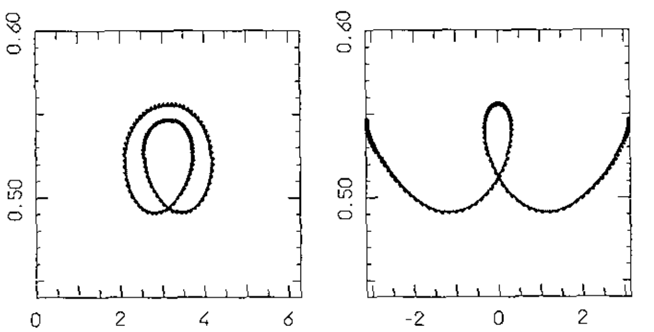

FIG. 12. The periodic orbit at the center of the three stable islands in the simulation at $J = 0.083 \times 10^{-3}$. On the left the coordinates are (q, N); on the right (q', N).

to 0.95. The solid line and the dashed line denote the stable and the unstable families of equilibrium points of the argument of perihelion. On the stable family, the argument of perihelion ω is equal to $\pi/2$ or $3\pi/2$; on the unstable one it is 0 or π. The two thick lines denote the position of the separatrices at $\omega = \pi/2$ between the ω-libration and ω-circulation regions ($\dot{\omega} < 0$ on the left and $\dot{\omega} > 0$ on the right). The global dynamics are like that in Fig. 5. With respect to the 2/1 mean motion commensurability, we observe that the resonance of the argument of perihelion occurs at smaller eccentricity.

In the region of negative circulation of ω, we proceed in analyzing the dynamic effects of Jupiter's eccentricity and inclination. Neither the ν_5 nor the ν_6 resonances are present; both can be found only in the region of positive

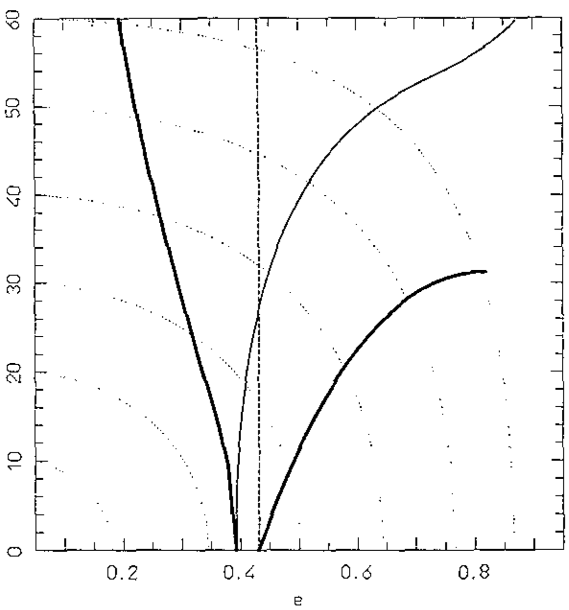

FIG. 13. Dynamics outside of the reference plane in the circular restricted problem. The same as Fig. 6.

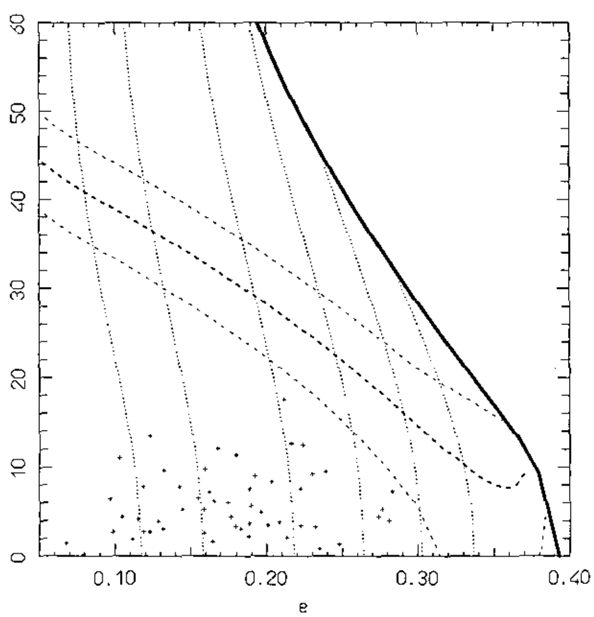

FIG. 14. The location of the ν_{16} resonance (bold dashed line) and its amplitude (thin dashed lines). The dotted curves denote some levels J'_ω = constant. The thick line is the separatrix of the ω-resonance. Crosses denote the asteroids of the Hilda group (osculating values).

circulation near the ω-separatrix, at $e > 0.45$. If we neglect Jupiter's eccentricity and consider only its inclination over the reference plane and the precession rate of its longitude of node, we get the scenario illustrated in Fig. 14. The dotted lines show the level curves of J'_ω; like in the case of the 2/1 commensurability, the values of e and i at $\omega = \pi/2$ evolve along these lines, as a consequence of the changes of N. The ν_{16} secular resonance, which forces large variations of N and therefore of the asteroid's inclination, is present in this portion of the space and is denoted by the bold dashed line. The two dashed lines on both its sides indicate the separatrices of the secular resonance.

A difference with respect to the 2/1 case is striking. The ν_{16} secular resonance is at larger eccentricity and inclination. Therefore, a large region of regular motion exists at moderate e and i. The asteroids of the Hilda group, denoted by crosses in Fig. 14, are all in this region. They escape the ν_{16} resonance, so that they do not have jumps in the inclination. Their critical angle $\Omega - \Omega_J$ circulates clockwise.

5. CONCLUSIONS

We have pointed out the relevant role of secular resonances inside the 2/1 and 3/2 mean motion commensurabilities. In particular, the interaction between ν_5 and ν_6 gives origin to a wide chaotic layer at large eccentricity. Conversely, the ν_{16} resonance, which pumps up the asteroid's inclination, is present at moderate eccentricity in the 2/1 and at larger eccentricity in the 3/2. Therefore, the distribution of the asteroids in the Hilda group (3/2 commensurability) is bounded by this secular resonance, which, on the contrary, would cross a fictitious family in the 2/1. This gives new hints for the possible explanation on the existence of the Hecuba gap and the Hilda group.

ACKNOWLEDGMENTS

We are very grateful to Ch. Froeschlé and H. Scholl for precious discussions and to S. Ferraz-Mello and P. Farinella for their help. We also thank J. Henrard for valuable suggestions.

REFERENCES

Ferraz-Mello, S. 1988. The high-eccentricity libration of the Hildas: Part I. *Astron. J.* **96,** 400–408.

Ferraz-Mello, S., and M. Sato, 1989. The very-high-eccentricity asymmetric expansion of the disturbing function near resonances of any order, *Astron. Astrophys* **225,** 541–547.

Henrard, J., and A. Lemaître 1983a. A second fundamental model for resonance. *Celest. Mech.* **30,** 197–218.

Henrard, J., and A. Lemaître 1983b. A mechanism of formation for the Kirkwood gaps. *Icarus* **55,** 482–494.

Henrard, J. 1988. Resonances in the planar elliptic restricted problem. In *Long Term Dynamical Behaviour of Natural and Artificial N-Body Systems* (A. E. Roy Ed.). Kluwer, New York.

Henrard, J. 1990. A semi-numerical perturbation method for separable Hamiltonian systems. *Celest. Mech.* **49,** 43–67.

Kneževič, Z., A. Milani, P. Farinella, Ch. Froeschlé, and C. Froeschlé 1991. Secular resonances from 2 to 50 AU *Icarus* **93,** 316–330.

Lemaître, A. 1984. High order resonances in the restricted three body problem. *Celest. Mech.* **32,** 109–126.

Lemaître, A., and J. Henrard 1990. On the origin of chaotic motion in the 2/1 Jovian resonance. *Icarus* **83,** 391–409.

Lemaître, A. 1992. Proper elements: What are they? In *Qualitative and Quantitative Behavirour of Planetary Systems* (R. Dvorak and J. Henrard, Eds.). Kluwer, New York, in press.

Lemaître, A., and A. Morbidelli 1992. Calculation of proper elements for high inclined asteroidal orbits by Henrard's semi-numerical method. Submitted for publication.

Michtchenko, T., and S. Ferraz-Mello 1992. The high-eccentricity libration of the Hildas: Part II. In *Qualitative and Quantitative Behaviour of Planetary Systems* (R. Dvorak and J. Henrard, Eds.), Kluwer. In press.

Moons, M., and J. Henrard 1992. Surfaces of section in the Miranda–Umbriel 3:1 inclination problem. Submitted for publication.

Moons, M., and A. Morbidelli 1992. The main mean motion commensurabilities in the planar circular and elliptic problem. In *Interactions between Physics and Dynamics of Solar System Bodies*, special issue of *Celest. Mech.*, in press.

Morbidelli, A., and A. Giorgilli 1990. On the dynamics in the asteroid belt. Part I and II. *Celest. Mech.* **47,** 145–204.

Morbidelli, A., and J. Henrard 1991. Secular resonances in the asteroid belt: Theoretical perturbation approach and the problem of their location. *Celst. Mech.* **51,** 131–167.

Morbidelli, A., and J. Henrard 1991. The main secular resonances ν_6, ν_5 and ν_{16} in the asteroid belt. *Celest. Mech.* **51,** 169–197.

Morbidelli, A. 1992. On the successive elimination of perturbation harmonics. *Celest. Mech.* **55,** 101–130.

Nakai, H., and H. Kinoshita 1985. Secular perturbations of asteroids in secular resonances. *Celest. Mech.* **36,** 391–407.

Nobili, A., A. Milani, and M. Carpino 1989. Fundamental frequencies and small divisors in the orbits of the outer planets. *Astron. Astrophys.* **210,** 313–336.

Poincaré H. 1892. *Les Méthodes Nouvelles de la Mécanique Céleste.* Gauthier–Villars, Paris.

Szebehely, V. 1967. *Theory of Orbits.* Academic Press, San Diego.

Williams, J. G. 1969. *Secular Perturbations in the Solar System* Ph.D. dissertation, University of California, Los Angeles.

Williams, J. G., and J. Faulkner 1981. The position of secular resonance surfaces. *Icarus* **46,** 390–399.

Wisdom, J. 1983. Chaotic behavior and the origin of the 3/1 Kirkwood gap. *Icarus* **63,** 272–289.

Wisdom, J. 1985. A perturbative treatment of the motion near the 3/1 commensurability, *Icarus* **63,** 279–282.

Yoshikawa, M. 1987. A simple analytical model for the ν_6 resonance. *Celest. Mech.* **40,** 233–272.

Yoshikawa, M. 1989. A survey on the motion of asteroids in commensurabilities with Jupiter *Astron. Astrophys.* **213,** 436–458.

Yoshikawa, M. 1991. Motions of asteroids at the Kirkwood gaps. II. On the 5:2, 7:3, and 2:1 resonances with Jupiter, *Icarus* **92,** 94–117.